Theoretical Energy and Exergy Analyses of Direct Methanol Fuel Cell

Joseph A.J[1], Abdulkareem A.S[2], Jimoh A[3], Afolabi A.S[*4]

[1,2,3]Chemical Engineering, School of Engineering and Engineering Technology, Federal University of Technology, PMB 65, Gidan Kwano, Minna, Niger State, Nigeria

[4]Department of Chemical, Metallurgical and Materials Engineering, College of Engineering, Botswana International University of Science and Technology, Palapye, Botswana

[1]juliusjaj@yahoo.com; [2]kasaka2003@futminna.edu.ng; [3]fatai2011@yahoo.com; [*4]afolabia@biust.ac.bw

Abstract-**This study studied the energy and exergy of direct methanol fuel cell (DMFC) through computer-assisted simulations. This was achieved through the development of mathematical models that represented the performance of a DMFC followed by simulations with a developed model using MATLAB. It was discovered that the simulated results conformed to the literature values with a correlation coefficient of 0.99 and standard deviation of 0.12. Simulations conducted with the developed model regarding the influence of operating parameters on the performance of the fuel cell indicated that maximum cell output voltage was obtained at a methanol concentration of 2 M. The results also showed that increases in temperature and operating pressure influenced the performance of the fuel cell. From the simulation results, it was seen that the maximum attainable energy efficiency of 95% was obtained at an operating temperature of 353 K, anode pressure of 1 atm, cathode pressure of 15 atm, and methanol concentration of 2 M, while the maximum exergy efficiency of 42% was obtained at the same parameters. It can therefore be inferred from the simulated results that improved performance, energy, and exergy efficiencies of a DMFC can be obtained by operating at controlled methanol concentrations and at temperatures that do not favour methanol cross-over or activation and concentration losses. Operating at a cathode pressure that is higher than the anode pressure can also enhance the performance of a fuel cell. Simulated results showed that cell performance depended on operating conditions; however, care must be taken in actual use, as high operating pressure will affect the safety and cost of operation of the cell because auxiliary equipment will be required to operate the cell at higher pressure.**

Keywords- Computer Simulation; Energy and Exergy; Mathematical Modeling; Methanol Fuel Cell

I. INTRODUCTION

The bulk of the energy utilized in manufacturing and residential applications typically comes from a single source, fossil fuel [1]. Fossil fuel reserves are quite limited and unevenly distributed throughout the world, and are also depleting rapidly. With time, the global demand for energy will outpace the resources [2]. In addition to the limited amounts of fossil fuel, traditional power generation, which uses heat engines based on the combustion of fossil fuels, gives off unhealthy gases such as CO_2, CO, SO_2, and NO_2 [3]. These emissions contribute to the degradation of the surrounding atmosphere and pose serious health problems to human and animals [4].

Power generation based on wind, waves, solar, water energy, etc. have all been applied as alternatives for steam or gas turbine power generation. Unfortunately, they are subject to seasonal and non-uniform production of energy and methods for harnessing their power are yet to be perfected [5]. Batteries and super-capacitors are alternative energy storage devices that are also available. However, the chemical substance or compound stored within it during manufacturing militates against their wide acceptance [5]. The important attribute of fuel cells compared to combustible fuels is the fact that when fossil fuels are utilized in burning engines to produce power, a large portion of the power from combustion is lost to heat and friction. This results in low efficiency of the engine. Conversely, since there are no moving parts within the fuel cell, friction and heat are greatly reduced and little maintenance is required [6]. Aside from efficiency, some fuel cells produce minute emissions due to their mechanism of operation [4]. A projection of the United States Department of Energy (UDE) indicates that if 15% of road vehicles used in America were powered by fuel cells, atmospheric emissions would be reduced by one million tons per year. Furthermore, greenhouse gas production would be reduced by 60 million tons [6]. Hence, high efficiency and little or no injurious emissions, based upon the brand of fuel utilized, are the principal benefits of fuel cells compared to internal combustion engines. The recognition that fuel cell technologies, especially DMFCs, as a non-harmful source of power that can compete well as an obtainable source of power, is still not known by the general public [7].

High costs and monopolies of fuel cell technologies have been identified as the major factors hindering the availability and commercialization of fuel cells [8]. How to reduce the high costs of membranes, field plates, and electrodes need to be resolved before fuel cells can be technologically and commercially viable [9]. Direct methanol fuel cells are a preferable alternative energy source because of the absence of storage systems that are typical of other types of fuel cells [5]. The fact that methanol is more dense than gasoline makes it easier to transport methanol safely without major adjustments to the current infrastructure used for gasoline transportation [5]. It has also been discovered that methane and methanol yield the lowest carbon dioxide production among hydrocarbons (ethane and ethanol) due to the high hydrogen to carbon ratio of their molecular structure [5].

DOI: 10.5963/AMSA0403001

Therefore, this study was motivated by the advancement and utilization of DMFCs, which can reduce the quantity of greenhouse gases emitted into the environment caused by typical fuel cells. A DMFC is an electrochemical mechanism that converts energy from a chemical reaction directly into electricity, with heat and CO_2 as by-products. DMFC utilizes direct methanol derived from a renewable source. The development of fuel cells is not commercially obtainable despite the fact that they have been recognized as ideal substitute to other energy sources such as petroleum, natural gas, coal and uranium. Shrestha and Mohan [10] investigated important issues that have hindered the development of commercial DMFCs. The results of their findings revealed that low power density and methanol crossover through the proton exchange membrane (PEM) are major factors responsible for the non-availability of DMFCs in commercial quantities. Low energy concentration at the anode is caused by sluggish electrochemical oxidation of the methanol, and methanol/CH_3OH cross-over hampers movement on the cathode catalyst.

Ayoub and Kazim [11] suggested that slow electro-oxidation kinetics requires the development of new electro-catalysts that can reduce catalyst poisoning. The catalyst should boost the pace of the reaction, and at the same time have improved activity in the direction of the CO_2 creation. Increasing cathode pressure and having a low methanol concentration can limit methanol cross-over at the anode [11]. On the anode side, feed channel patterns should be modified to facilitate the rapid elimination of CO_2, and according to Lu and Wang [12], small and homogeneously spread pores of feed channel patterns produce uniform pour rather than strike pour. The CO_2 produced by DMFCs can be captured by the utilization of algae [12] or by other more established techniques such as carbon capture and storage (CCS) and artificial tree systems/methods in which the captured CO_2 can be used in methanol synthesis [12]. Neja, et al. (2014) [13] reported a method of theoretically calculating exergy efficiency of the proton exchange membrane fuel cell driven with methanol, and validated their results with experimental values. The effects of temperature and pressure on the efficiency of a DMFC were investigated and results revealed that energy efficiency of a fuel cell rises with increases in operating temperature and pressure. The present study reported on the development of a predictive model for the performance of DMFCs in regards to operating parameters like temperature, pressure, concentration of fuel, and flow rate of oxidants in addition to the influence of operating parameters on the energy and exergy efficiency of DMFCs.

Jin and Nyuyen [14] described exergy as a functional work potential of a given quantity of power at a particular position. The operating potential of the power in a device at a particular condition, compared to a position, is the highest functional work that can be obtained from a system. The energy analysis for any system can be established using the first law of thermodynamics, although the law only provides information about the quantity of energy produced [14]. However, the second law, which involves exergy analysis, considers the quality of energy produced and deals with energy degradation in a process. Hence, the quest in this research was to build an analytical mathematical replica of the power that could be given as output by the device as a function of its operating conditions. The study also aimed to simulate a developed model and find interactions among the operating conditions that affected the quantity of energy formed by a fuel cell powered by methanol.

II. CONCEPTUALIZATION OF THE MODELING TECHNIQUE

The model was divided into exergy, heat (thermal model), and electrochemical analysis. The subsequent postulations considered during the conceptualization of the model included the following:

(1) Ohmic, activation, and concentration polarization were the overpotentials (losses) encountered in the DMFC.

(2) Reaction in the fuel cell was partial (incomplete).

(3) Heat lost in the system occurred by natural convection, forced convection, and radiation.

(4) Calculation of enthalpies in the fuel cell for each stream was based on standard temperature.

A. Page Layout

The anode and cathode reactions were described by the following equations (Yachi, *et al*) [5]:

$$Anode: \quad CH_3OH + H_2O \rightarrow CO_2 + 6H^+ + 6e^- \qquad E^o = 0.02V$$

$$Cathode: \quad \frac{3}{2}O_2 + 6H^+ + 6e^- \rightarrow 3H_2O \qquad E^o = 1.23V$$

$$Overall: \quad CH_3OH + \frac{3}{2}O_2 \rightarrow CO_2 + 2H_2O \qquad E^o = 1.21V$$

The net (or actual) voltage output of the DMFC, E_{cell} as related to the thermodynamically predicted voltage of the fuel cell and voltage losses, was expressed in [10] as:

$$E_{cell} = E_{OCV} - (\eta_{act} + \eta_{ohmic} + \eta_{conc}) \tag{1}$$

DOI: 10.5963/AMSA0403001

where E_{OCV} is the reversible cell voltage (also called thermodynamic equilibrium potential or open circuit voltage). η_{conc}, η_{act}, and η_{ohmic} are concentration (or mass transport), activation, and ohmic losses of the cell, respectively. These losses are also known as overvoltages; they represent the voltage drop.

Parsons (2000) [15] expressed thermodynamic potential as the utmost electrical energy attained by a fuel cell at thermodynamic stability. The thermodynamic potential can be obtained from the Nernst equation [15] with the following:

$$E_{OCV} = E^{\circ} + \frac{RT}{nF} ln\left[\frac{p_{CH_3OH}\left(p_{O_2}\right)^{1.5}}{p_{CO_2}\left(p_{H_2O}\right)^{2}}\right] \tag{2}$$

where E^0 is the set state position potential (1 atm and 298.15 K); p_{O2} and p_{CH3OH} are limited pressures of oxygen with methanol, correspondingly; n represents the amount of moles of transferred electrons; F *is* 96,485 C/mole, which is the Faraday constant; R is 8.314J/mole K, which is the universal gas constant; and T is temperature (^{o}K).

From Eq. (1), it can be deduced that the output voltage is less than the thermodynamic potential due to irreversible losses. Using an empirical approach, Shrestha and Mohan [10] proposed the following empirical equations for the determination of activation, ohmic, and concentration losses in a DMFC:

$$\eta_{act} = A\ln(i) + C_2 \tag{3}$$

$$\eta_{ohmic} = iR + C_1 \tag{4}$$

$$\eta_{conc} = m \times e^{(ni)} \tag{5}$$

where A, R, m, and n are the empirical coefficients and C_1 and C_2 are constants, and i is the current strained out of the device. The empirical coefficients plus the constants can be estimated from the following second-order polynomials [10]:

$$C_1 = 0.0302M^2 - 0.1331M + 0.4088 \tag{6}$$

$$R = -0.223M^2 + 0.9393M + 0.0202 \tag{7}$$

$$A = -0.0011M^2 + 0.0041M - 0.0079 \tag{8}$$

$$C_2 = -0.0026M^2 + 0.0085M + 0.1782 \tag{9}$$

$$m = 0.1325M^2 - 0.5682M + 1.4602 \tag{10}$$

$$n = -0.3108M^2 + 1.5651M + 4.8193 \tag{11}$$

where M is the molar concentration of methanol fuel. Substituting Eqs. (6) through (11) into Eqs. (3) through (5) to obtain the activation, ohmic, and concentration losses as a function of concentration and current becomes as follow:

$$\eta_{act} = (-0.0011M^2 + 0.0041M - 0.0079)\ln(i) + (-0.0026M^2 + 0.0085M + 0.1782) \tag{12}$$

$$\eta_{ohmic} = i(-0.223M^2 + 0.9393M + 0.0202) + (0.0302M^2 - 0.1331M + 0.4088) \tag{13}$$

$$\eta_{conc} = (0.1325M^2 - 0.5682M + 1.4602) \times e^{i\left(-0.3108M^2 + 1.5651M + 4.8193\right)} \tag{14}$$

Putting Eqs. (12) to (14) into Eq. (1), the net voltage of DMFC can now be evaluated as

$$\begin{aligned} E_{cell} = {} & \left\{E^{\circ} + \frac{RT}{nF} ln\left[\frac{p_{CH_3OH}\left(p_{O_2}\right)^{1.5}}{p_{CO_2}\left(p_{H_2O}\right)^{2}}\right]\right\} \\ & - \{(-0.0011M^2 + 0.0041M - 0.0079)\ln(i) + (-0.0026M^2 + 0.0085M + 0.1782)\} \\ & - \{i(-0.223M^2 + 0.9393M + 0.0202) + (0.0302M^2 - 0.1331M + 0.4088)\} \\ & - \left\{(0.1325M^2 - 0.5682M + 1.4602) \times e^{i\left(-0.3108M^2 + 1.5651M + 4.8193\right)}\right\} \end{aligned} \tag{15}$$

Eq. (15) is the model equation representing the output voltage from DMFC as a function of operating conditions designed for a single fuel cell. The output voltage from Eq. (15) can be used to calculate the electrical energy dissipated by multiplying overall cell-voltage by the current (I) and duration of operation (t).

The DMFC efficiency can be obtained from Eq. (16) [1]:

$$Cell\ efficiency = \frac{E_c}{E_{cell}} \times 100 = \frac{1.21}{E_{cell}} \times \frac{100}{1} \tag{16}$$

where E_c represents the real voltage rate with a value of 1.21 V [5], and E_{cell} is the predictive cell voltage obtained from the developed model.

DOI: 10.5963/AMSA0403001

In practice, complete oxidation of methanol (fuel) does not take place in the fuel cell, which implies that not all reactants are transformed into products; some remain as reactants and are converted into other products. Little fractions of the reactants pass through the device without taking part in the reaction that produces energy. Therefore, a fuel utilization term is set up for calculating DMFC efficiency [15]. The fuel utilization term is given as:

$$\delta_f = \frac{mass\ of\ fuel\ methanol\ reacted\ in\ the\ cell}{mass\ of\ fuel\ methanol\ input\ into\ the\ cell} \tag{17}$$

Substituting Eq. (17) into (16) gives:

$$Cell\ efficiency = \delta_f \frac{E_c}{E_{cell}} \times 100 \tag{18}$$

B. The DMFC Mass Balance

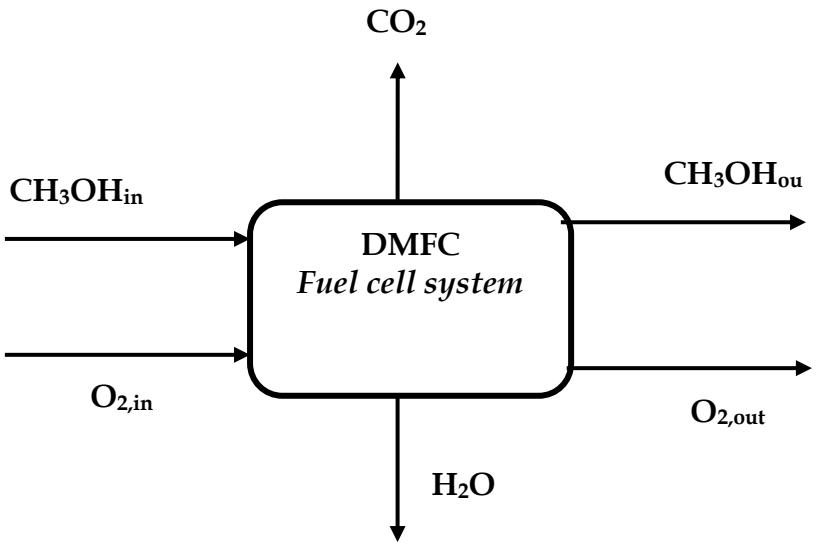

Fig. 1 Schematic mass balance for DMFC

The appropriate calculations of DMFC efficiency and thermal energy analysis are based on mass balance equations that rely on the law of conservation of mass (see Fig. 1) from the assumption that the reaction in the cell is incomplete, i.e. not every reactant put in the device is utilized.

$$m_{CH3OH,in} = m_{CH3OH,react} + m_{CH3OH,out} \tag{19}$$

$$m_{O2,in} = m_{O2,react} + m_{O2,out} \tag{20}$$

where $m_{O2,in}$ and $m_{CH3OH,in}$ are the rates of mass flow of oxygen and methanol into the cell, and $m_{O2,out}$ and $m_{CH3OH,out}$ are the rates of mass flow of oxygen and methanol out of the cell. At the anode side of the cell, the rate of consumption of methanol is obtained as shown in Eq. (21) [16]:

$$m_{CH3OH,react} = \zeta_A M_{CH3OH} \frac{JA_{cell}}{6F} \times 10^{-3} \tag{21}$$

where A_{cell} is the effective area of the cell, M_{CH3OH} is the molecular weight of methanol, J is current density, ζ_A stands for anode stoichiometry coefficient, and F is Faraday's constant.

Similarly, the mass of oxygen that reacted at the cathode side is:

$$m_{O2,react} = \zeta_C M_{O2} \frac{JA_{cell}}{6F} \times 10^{-3} \tag{22}$$

while the mass of H_2O and CO_2 formed in the DMFC can be evaluated as follows [16]:

$$m_{H2O,out} = M_{H2O} \frac{JA_{cell}}{6F} \times 10^{-3} \tag{23}$$

$$m_{CO2,out} = M_{CO2} \frac{JA_{cell}}{6F} \times 10^{-3} \tag{24}$$

where M_{CO2} and M_{H2O} are the molecular weights of CO_2 and H_2O, respectively.

DOI: 10.5963/AMSA0403001

The masses of methanol and oxygen out of the cell can be calculated using the relationship presented in Eqs. (25) and (26), respectively.

$$m_{CH3OH,in} = m_{CH3OH,react} + m_{CH3OH,out}$$
$$m_{CH3OH,out} = m_{CH3OH,in} - m_{CH3OH,react} \quad (25)$$

$$m_{O2,in} = m_{O2,react} + m_{O2,out}$$
$$m_{O2,out} = m_{O2,in} - m_{O2,react} \quad (26)$$

Substituting Eqs. (21) and (22) into Eqs. (25) and (26) to obtain Eqs. (27) and (28):

$$m_{CH3OH,out} = m_{CH3OH,in} - \zeta_A M_{CH3OH} \frac{JA_{cell}}{6F} \times 10^{-3} \quad (27)$$

$$m_{O2,out} = m_{O2,in} - \zeta_C M_{O2} \frac{JA_{cell}}{6F} \times 10^{-3} \quad (28)$$

C. Energy Analysis of DMFC

The law of energy conservation was employed for the DMFC energy analysis and thermal path flow. A heat flow diagram is shown in Fig. 2.

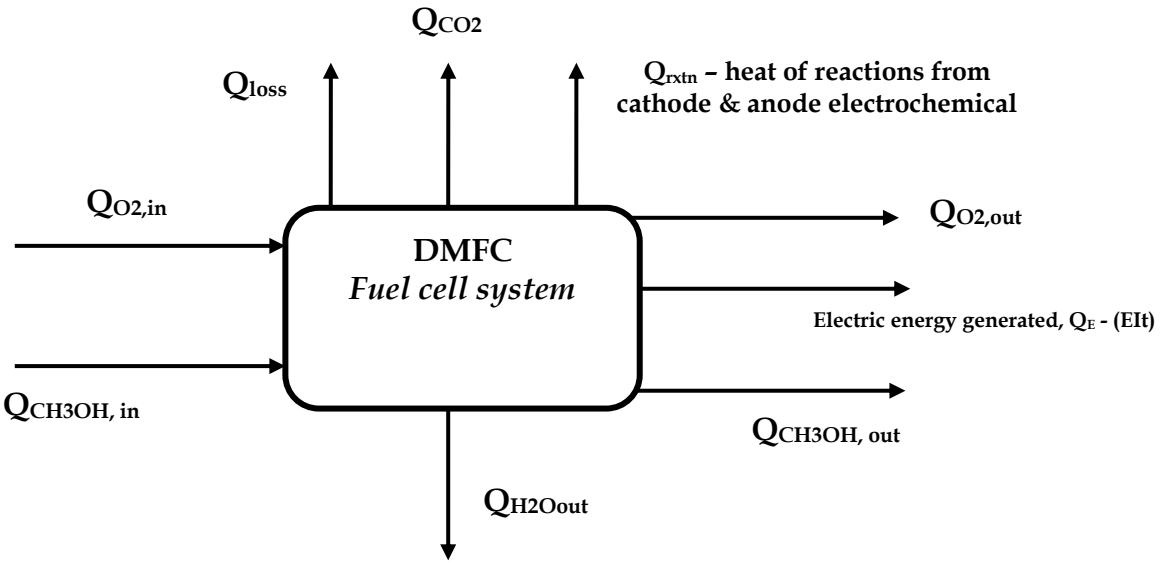

Fig. 2 Schematic heat balances for DMFC

The energy balance for the cell, as shown in Fig. 2, can be broken down into:

$$Q_{input} - Q_{output} - Q_{acc} = 0 \quad (29)$$

where Q_{output} = heat output from the cell, Q_{input} = heat input from the cell, and Q_{acc} = heat accumulated in the cell.

Assuming that $Q_{net} = Q_{acc}$ and rearranging Eq. (29) gives the following:

$$Q_{net} = Q_{input} - Q_{output} \quad (30)$$

From Fig. 2, the heat input into the system is obtained with:

$$Q_{input} = Q_{CH_3OH,in} + Q_{O_2in} \quad (31)$$

Similarly, heat out of the cell is obtained with:

$$Q_{output} = Q_{CH_3OHout} + Q_{O_2out} + Q_{H_2O} + Q_{CO_2} + Q_{rxtn} + Q_E + Q_{loss} \quad (32)$$

Furthermore, heat is carried away in a number of ways from the device heap by the manufactured gases and water. Lost heat from the device, Q_{loss}, is expressed with the following:

$$Q_{loss} = Q_{nc} + Q_{fcn} + Q_{rad} \quad (33)$$

DOI: 10.5963/AMSA0403001

where Q_{rad} Q_{nc}, and Q_{fcn} are losses of heat by means of radiation, natural convection, and forced convection, respectively. The heat loss by convection (natural and forced) can be evaluated from the relationship shown in Eqs. (34) and (35), respectively:

$$Q_{nc} = h_{nc}A_{FC}(T_{FC} - T_0) \tag{34}$$

$$Q_{fcn} = m_{coolant}C_{p,air}\left(T_{coolant,out} - T_0\right) \tag{35}$$

The heat loss by radiation can be evaluated from Eq. (36), assuming that the cell is a nonblack surface (Assumption 3), the heat loss is by natural convection, forced convection, or radiation, and hence heat loss from the cell can be represented by the relationship shown in Eq. (36). For nonblack surfaces, the Stefan-Boltzmann law gives the emitted energy flux at temperature *T*, as shown in Eq. (36) [17]:

$$Q_{rad} = \varepsilon\sigma A_{FC}({T^4}_{FC} - {T^4}_0) \tag{36}$$

where, σ = 5.67 x 10^{-8} W/m^2 K^4 (Stefan-Boltzmann constant), A_{FC} = surface area of the cell, T_{FC} = cell temperature, ε = emissivity factor, and T_0 = environmental temperature.

Substituting Eqs. (31) through (36) into Eq. (30) yields:

$$\begin{aligned} Q_{net} = Q_{CH_3OH,in} + Q_{O_2in} - Q_{CH_3OHout} - Q_{O_2out} - Q_{H_2O} - Q_{CO_2} - Q_{rxtn} - Q_E - h_{nc}A_{FC}(T_{FC} - T_0) \\ - m_{coolant}C_{p,air}\left(T_{coolant,out} - T_0\right) - \varepsilon\sigma A_{FC}({T^4}_{FC} - {T^4}_0) \end{aligned} \tag{37}$$

Eq. (37) can be written in terms of enthalpy, as shown in Eq. (38):

$$\begin{aligned} Q_{net} = \Delta H_{CH_3OH,in} + \Delta H_{O_2in} - \Delta H_{CH_3OH,out} - \Delta H_{O_2out} - \Delta H_{H_2O} - \Delta H_{CO_2} - \Delta H_{rxtn} - Q_E - h_{nc}A_{FC}(T_{FC} - T_0) \\ - m_{coolant}C_{p,air}\left(T_{coolant,out} - T_0\right) - \varepsilon\sigma A_{FC}({T^4}_{FC} - {T^4}_0) \end{aligned} \tag{38}$$

where ΔH_{CH_3OH}, ΔH_{H_2O}, ΔH_{CO_2} and ΔH_{O_2} are the enthalpies of methanol, water, CO_2, and oxygen, respectively. The enthalpy of the reaction is ΔH_{rxtn}. Ecell is the net output voltage of Q_E, which is the electrical energy produced by the cell, and can be represented as:

$$Q_E = E_{cell} \times It \tag{39}$$

Eq. (38) then becomes:

$$\begin{aligned} Q_{net} = \Delta H_{CH_3OH,in} + \Delta H_{O_2in} - \Delta H_{CH_3OH,out} - \Delta H_{O_2out} - \Delta H_{H_2O} - \Delta H_{CO_2} - \Delta H_{rxtn} - E_{cell}It \\ - h_{nc}A_{FC}(T_{FC} - T_0) - m_{coolant}C_{p,air}\left(T_{coolant,out} - T_0\right) - \varepsilon\sigma A_{FC}({T^4}_{FC} - {T^4}_0) \end{aligned} \tag{40}$$

Eq. (40) represents the mathematical model developed for the net heat generated by the direct methanol fuel cell at different operating parameters. The cell energy efficiency can be evaluated based on the relationship shown in Eq. (41) [16]:

$$\eta_{energy,system} = \frac{\hat{W}_{net}}{HHV_{CH3OH} \times m_{CH3OH,in}} \tag{41}$$

HHV_{CH3OH} = higher heating value of methanol, and $m_{CH3OH,in}$ is the mass flow rate of methanol into the system.

D. Exergy Analysis of DMFC

The specific exergy (J/kg) is the summation of thermo mechanical exergy, potential exergy, and kinetic exergy, as shown in Eq. (42).

$$e = e_{ke} + e_{pe} + e_{tm} \tag{42}$$

where $e = \frac{\hat{E}}{m}$, $\hat{E}$ = rate of total exergy (J/hr), and *m* is the rate of mass flow (kg/hr).

The total exergy is given by the relationship shown in Eq. (43):

$$\hat{E} = m\left(e_{ke} + e_{pe} + e_{tm}\right) \tag{43}$$

$$\hat{E} = me_{ke} + me_{pe} + me_{tm} \tag{44}$$

And based on exergy rates, the following is true:

$$\hat{E} = \hat{E}_{ke} + \hat{E}_{pe} + \hat{E}_{tm} \tag{45}$$

The exergy of specific kinetic energy term e_{ke} can be written as:

$$e_{ke} = \frac{1}{2}v^2 \tag{46}$$

DOI: 10.5963/AMSA0403001

The exergy of specific potential energy term e_{pe} can be written as:

$$e_{pe} = gZ \tag{47}$$

where g is the gravitational acceleration of Earth (m/s^2) and Z is the flow elevation higher than sea level (m). The thermo mechanical (or specific physical) exergy is based on temperature and pressure, and at a given state can be defined as follows:

$$e_{tm} = e^{PH} = (h - h_0) - T_0(s - s_0) \tag{48}$$

where s_0 is the specific entropy (J/kg) and h_0 is the specific enthalpy (J/kg.K) evaluated at standard situations, correspondingly. Hence, $(s\text{-}s_0)$ is the change in entropy (Δs) and $(h\text{-}h_0)$ is the change in enthalpy (Δh). Substituting the terms for exergy rates from Eqs. (46) through (48) into Eq. (44) yields an expression for the total exergy rate in Eq. (49):

$$\hat{\mathrm{E}}^{PH} = \frac{1}{2}mv^2 + mgZ + m[(h - h_0) - T_0(s - s_0)\ ] \tag{49}$$

The specific physical exergy term, which is shown in Eq. (49) above, can be further analyzed from:

$$e^{PH} = (h - h_0) - T_0(s - s_0) \tag{50}$$

where s_0 and h_0 indicate the specific entropy and enthalpy estimated at standard situations, respectively. The specific enthalpy and entropy changes Δh, $(h\text{-}h_0)$, and Δs, $(s\text{-}s_0)$ can each be represented as follows [18, 19]:

$$(h - h_0) = \int_{T_0}^{T} C_p(T)dT = C_p(T - T_0) \tag{51}$$

$$(s - s_0) = \int_{T_0}^{T} \frac{C_p}{T}dT - \int_{P_0}^{P} \left(\frac{\partial V}{\partial T}\right)dP \tag{52}$$

From Eq. (51), assuming that the system obeys the ideal gas law, PV = RT; then the following is true:

$$\frac{V}{T} = \frac{R}{P} \tag{53}$$

where the universal gas constant is R, and substituting that into Eq. (52), the following is obtained:

$$(s - s_0) = \int_{T_0}^{T} \frac{C_p}{T}dT - \int_{P_0}^{P} \left(\frac{R}{P}\right)dP \tag{54}$$

Integrating Eq. (54) obtains the following:

$$(s - s_0) = C_p \ln\left(\frac{T}{T_0}\right) - R \ln\left(\frac{P}{P_0}\right) \tag{55}$$

Both types of specific heat (at constant volume C_v and at constant pressure C_p) are linked to R in the following manner:

$$C_p = C_v + R \text{ or } R = C_p - C_v$$

Substituting for R in Eq. (55) obtains:

$$(s - s_0) = C_p \ln\left(\frac{T}{T_0}\right) - (C_p - C_v) \ln\left(\frac{P}{P_0}\right) \tag{56}$$

Re-arranging Eq. (56) obtains:

$$(s - s_0) = C_p \left[\ln\left(\frac{T}{T_0}\right) - \left(1 - \frac{C_v}{C_p}\right) \ln\left(\frac{P}{P_0}\right)\right] \tag{57}$$

Representing C_v/C_p with the specific heat ratio k where: $k = \frac{C_p}{C_v}$ or $\frac{1}{k} = \frac{C_v}{C_p}$, the following can be obtained:

$$(s - s_0) = C_p \left[\ln\left(\frac{T}{T_0}\right) - \left(1 - \frac{1}{k}\right) \ln\left(\frac{P}{P_0}\right)\right] \tag{58}$$

or

$$(s - s_0) = C_p \left[\ln\left(\frac{T}{T_0}\right) - \left(\frac{k - 1}{k}\right) \ln\left(\frac{P}{P_0}\right)\right] \tag{59}$$

DOI: 10.5963/AMSA0403001

Substituting Eqs. (51) and (59) into Eq. (50) gives an expression for the total physical exergy, as in the following:

$$e^{PH} = C_p(T - T_0) - T_0 C_p \left[\ln\left(\frac{T}{T_0}\right) - \left(\frac{k-1}{k}\right)\ln\left(\frac{P}{P_0}\right)\right] \tag{60}$$

or

$$e^{PH} = C_p T - C_p T_0 - C_p T_0 \left[\ln\left(\frac{T}{T_0}\right) - \left(\frac{k-1}{k}\right)\ln\left(\frac{P}{P_0}\right)\right] \tag{61}$$

Factorizing C_pT_0 out of the expression gives the expression for the specific heat ratio *k* and exergy physical of an ideal gas by means of constant specific heat C_p, as shown in Eq. (62):

$$e^{PH} = C_p T_0 \left[\frac{T}{T_0} - 1 - \ln\left(\frac{T}{T_0}\right) + \ln\left(\frac{P}{P_0}\right)^{\left(\frac{k-1}{k}\right)}\right] \tag{62}$$

Substituting the physical exergy term in Eq. (62) into Eq. (49) for total rate of exergy will give the following:

$$\hat{\mathrm{E}} = \frac{1}{2}mv^2 + mgZ + mC_pT_0\left[\frac{T}{T_0} - 1 - \ln\left(\frac{T}{T_0}\right) + \ln\left(\frac{P}{P_0}\right)^{\left(\frac{k-1}{k}\right)}\right] + \hat{\mathrm{E}}^{CH} \tag{63}$$

The chemical exergy of a substance, based on its chemical potentials, can be estimated from the relationship shown in Eq. (64):

$$\hat{\mathrm{E}}^{CH} = (\mu^0 - \mu_0^0) + RT_0 \ln\left(\frac{C}{C_0}\right) \tag{64}$$

Maher and Sadiq [18] expressed molar precise/specific chemical exergy of reference constituent *i* at hand in the surroundings on limited/partial pressure $P_{00,i}$ as:

$$e^{CH} = RT_0 \ln\left(\frac{P_0}{P_{00,i}}\right) \tag{65}$$

Substituting the expression for e^{CH} in Eq. (65) into Eq. (63) gives an overall total exergy rate that can be used to calculate the exergy for each of the components involved in the mathematical model:

$$\hat{\mathrm{E}} = \frac{1}{2}mv^2 + mgZ + mC_pT_0\left[\frac{T}{T_0} - 1 - \ln\left(\frac{T}{T_0}\right) + \ln\left(\frac{P}{P_0}\right)^{\left(\frac{k-1}{k}\right)}\right] + mRT_0 \ln\left(\frac{P_0}{P_{00,i}}\right) \tag{66}$$

For a DMFC system, the exergetic efficiency is defined as:

$$\varepsilon = \frac{Electrical\ Output}{(Exergy)_{Rxtnt} - (Exergy)_{Prdct}} \tag{67}$$

$$\varepsilon = \frac{\hat{\mathrm{W}}}{(\hat{\mathrm{E}}_{O_2,R} + \hat{\mathrm{E}}_{CH_3OH,R}) - (\hat{\mathrm{E}}_{CO_2,P} + \hat{\mathrm{E}}_{H_2O,P})} \tag{68}$$

Thus, Eq. (68) represents the predictive model for the exergetic efficiency of a DMFC.

III. RESULTS AND DISCUSSION

This study focused on the theoretical mathematical and computer simulations for direct methanol fuel cell performance under conditions of specific operating parameters such as methanol concentration, anode and cathode pressure, and operating temperature. The simulated results obtained are presented in Figs. 3-9.

Fig. 3 shows the comparative results of simulated data with literature values under similar operating conditions of methanol concentration of 2M, temperature of 353 K, pressure of 1 atmosphere, and methanol flow rate of 0.001 g/s. These results indicated that the open circuit voltage was at 0.477 V for the simulated results, while the literature value was 0.42 V. The open circuit voltage obtained from the literature and simulations were lower than that of a cell powered with hydrogen (proton exchange membrane fuel cell), which is in the range of 0.6 V to 0.8 V [10]. This variation can be attributed to the slower oxidation of methanol compared to hydrogen, and the possibility of crossover of methanol from the anode side to the cathode side [10, 20].

In order to validate the developed model of the DMFC, a polarization curve of the simulated results was compared to that of literature, as presented in Fig. 1. It can be observed from the results that the simulated results compared favorably to the

DOI: 10.5963/AMSA0403001

literature results. The slight variation between the simulated and literature results can be attributed to assumptions considered while conceptualizing the model. For instance, the crossover of the methanol from anode to cathode reduces the performance of the cell, which was not considered during the development of the model. The statistical analysis of both the literature and simulated results showed a correlation coefficient of 0.99 with a standard deviation of 0.12.

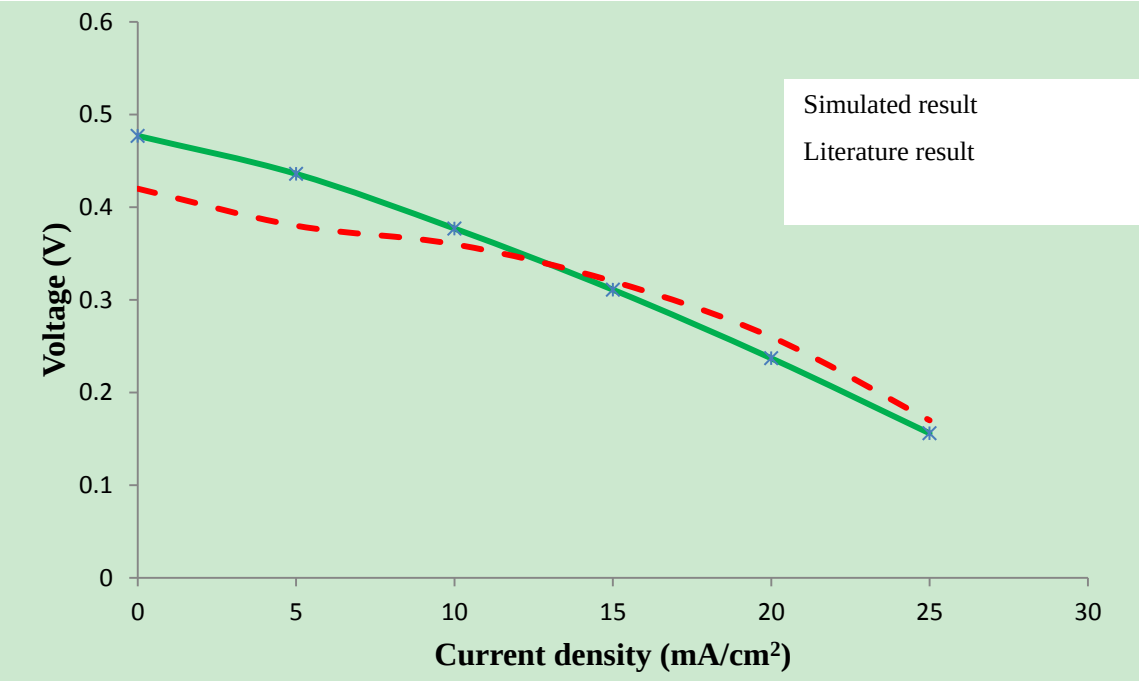

Fig. 3 Polarization curves of cell voltages for simulated and literature values

In order to examine the performance of the DMFC in various operating conditions, the developed model was subjected to diverse standards of input variables, such as methanol concentration, methanol inlet flow rate, operating temperature, and cathode and anode pressures, which are the main variables that determine the efficiency and performance of a DMFC [11]. The effects of these factors were investigated by simulation, and the results obtained are presented in Figs. 4 through 9. Fig. 4 presents the simulated influence of methanol concentration on cell performance.

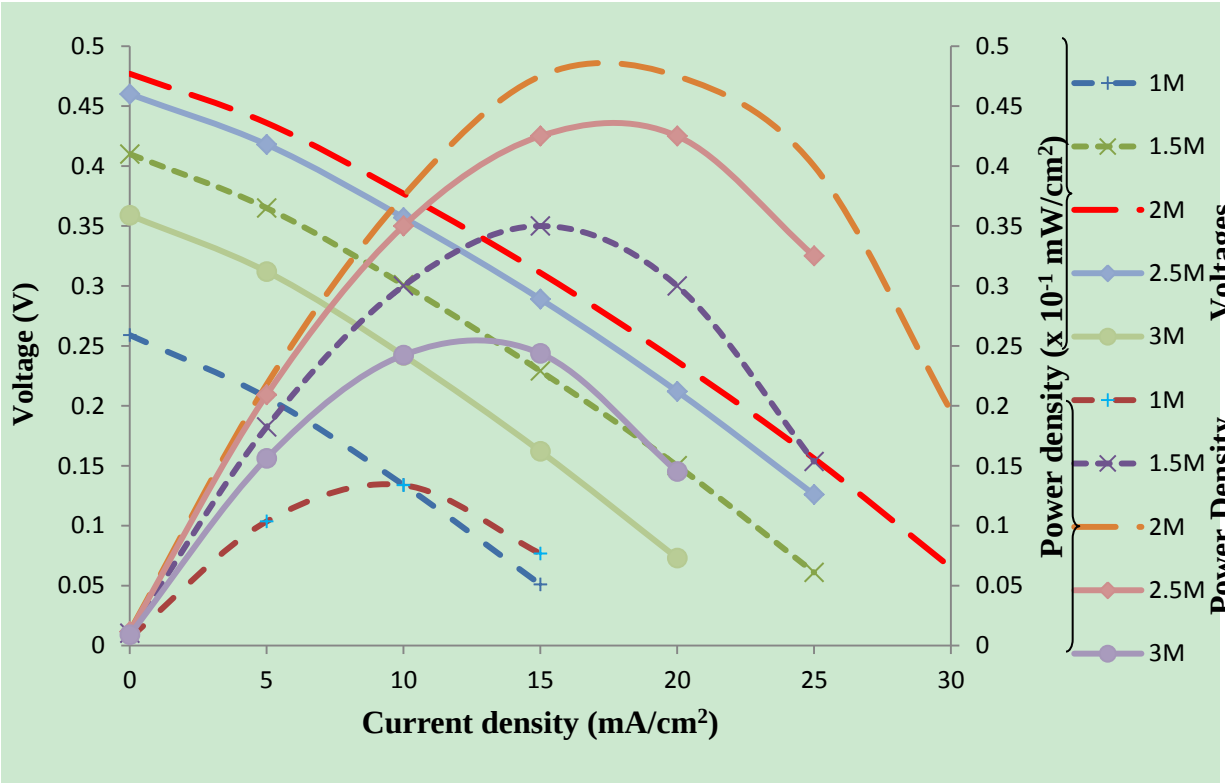

Fig. 4 Simulated effects of methanol concentration on the performance of DMFC

DOI: 10.5963/AMSA0403001

For the purpose of simulation of the predictive developed model, the methanol concentration was varied between 1 and 3 moles, with step increments of 0.5 mole. It can be observed from the results (Fig. 4) that both the output voltage and power density of the cell increased with increases in methanol concentration until the methanol concentration was at 2 moles. A further increment in the methanol concentration from 2.5 moles to 3 moles resulted in a decrease in the cell performance, as revealed in Fig. 4. This was an indication of the possibility of methanol crossover from anode to cathode through the membrane, which lead to a decline in the cell performance. Hence, a methanol concentration of 2 moles seemed to be the fuel concentration for best performance of a fuel cell powered with methanol.

Also simulated in this study was the influence of cathode and anode pressures on cell performance, and the results obtained are presented in Figs. 5 and 6, respectively. For the purpose of simulating the influence of electrode pressure on cell performance, the operating pressure was varied between 1 and 15 atmospheres. It was obvious from the results presented in Figs. 5 and 6 that both cathode and anode pressures had influence on the DMFC performance. The output voltage increased with increases in pressure from 1 to 15 atm. It is worth mentioning that the simulated results show increments in the cell performance with added pressure; however, care must be taken in real life operations to avoid operating the system at higher pressures of 10 and 15 atmospheres for safety and economic reasons. Operating at a higher pressure might require additional auxiliary equipment, which adds to the cost of fuel cell operation. The results also indicated that the effects of cathode pressure were more significant than those of anode pressure. The variation between the cathode and anode performances under the same operating conditions could be a result of the fact that the electrochemical oxidation of methanol to produce CO_2 takes place on the anode side. The CO_2 bubbles eventually block the anode channel, which result in limited transport and poor velocity distribution of the reactant.

The influence of operating temperature on the DMFC performance was simulated, and the results are presented in Fig. 7. The results showed that the output voltage and power density increased slightly when the operating temperature increased from 323 K to 423 K. The increment in the performance of the cell with the rise in temperature was attributed to the fact that the electrochemical reaction that produces energy in the cell required an effective collision between the molecules of the reactants, and the energy required from this collision was derived from the cell temperature. It is also worth mentioning that the simulated results positively favored cell performance, but care must be taken not to increase the cell temperature beyond the limit, which will result in drying of the proton exchange membrane of the cell and a consequent reduction in cell performance.

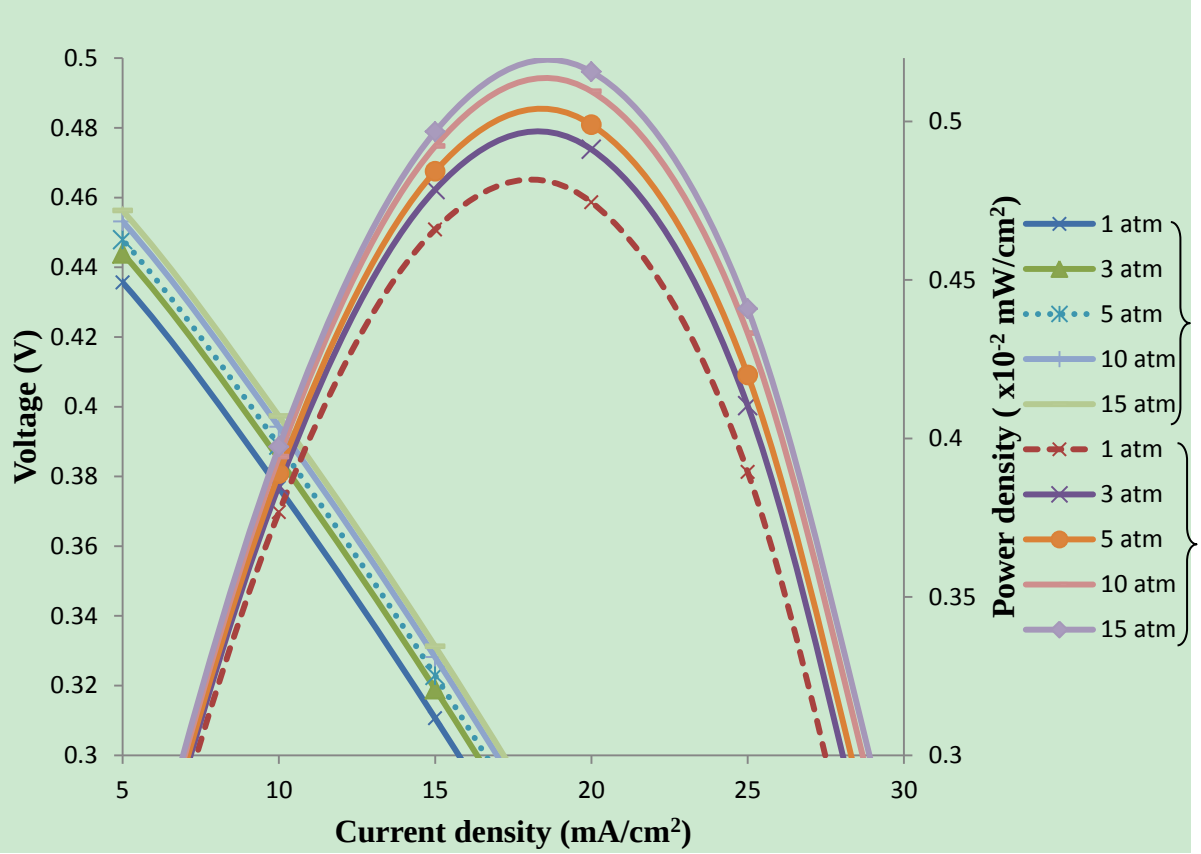

Fig. 5 Simulated effects of cathode pressure on DMFC performance

DOI: 10.5963/AMSA0403001

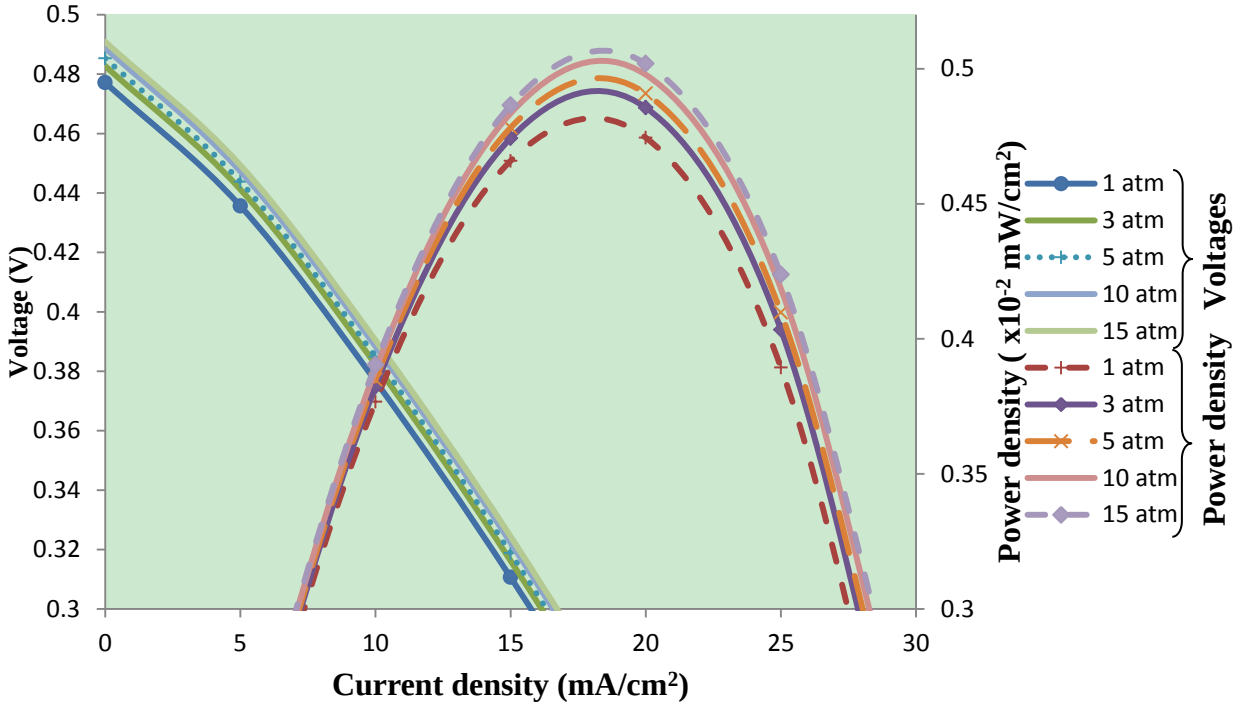

Fig. 6 Simulated effects of anode pressure on DMFC performance

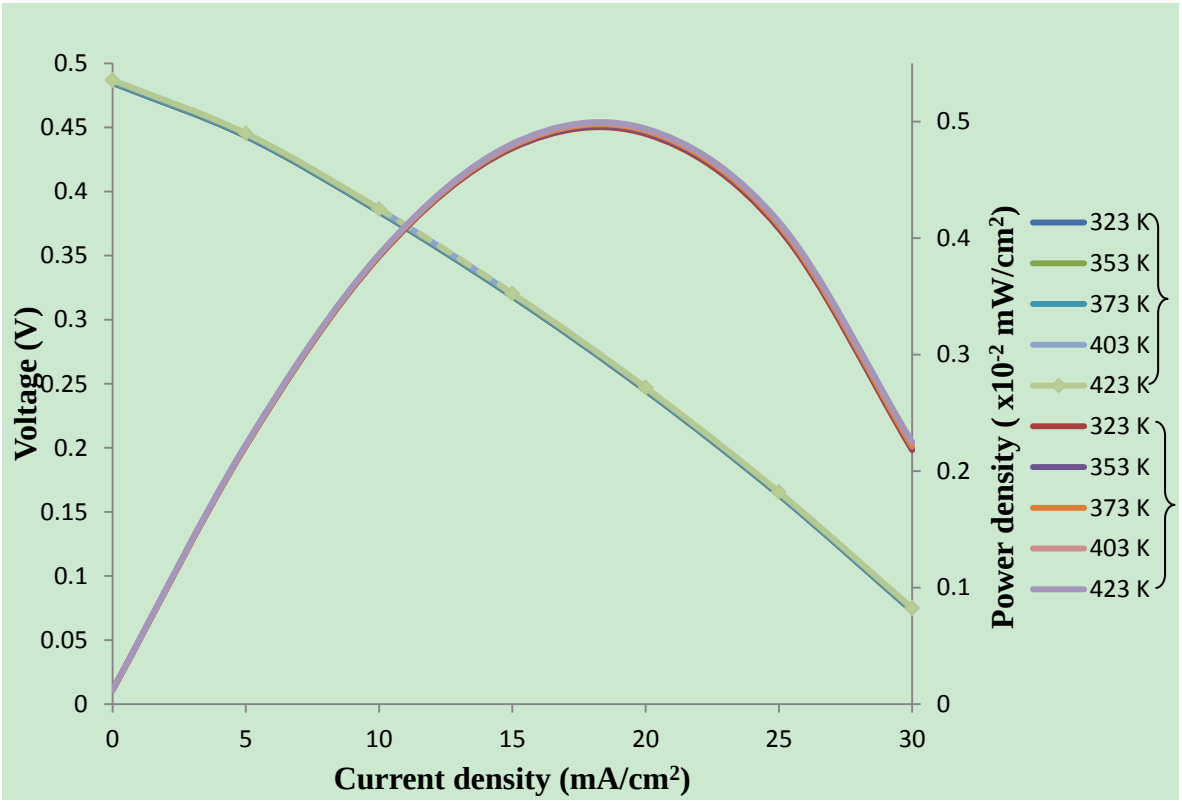

Fig. 7 Simulated effects of operating temperature on the DMFC performance

Also simulated in this study was the influence of operating parameters on the energy and exergy efficiency of the fuel cell. The simulated results on the influence of methanol concentration and current density on the energy and exergy performance of direct methanol fuel cell are presented in Figs. 8 and 9. The results shown in Fig. 8 indicated that the exergy efficiency of the DMFC decreased with increases in current density. This illustrated that the cell performance can be enhanced if voltage losses are greatly minimized because exergy efficiency will increase. Operating at high temperatures and appropriate anode and cathode pressures can reduce voltage losses. On the influence of current on energy efficiency of the cell, the simulated results (Fig. 8) indicated that the energy efficiency curve showed an initial increase as current density increased; it reached its

DOI: 10.5963/AMSA0403001

maximum and then decreased continuously. This fall in efficiency after reaching its peak was attributed to methanol crossover, which increased considerably with increases in current density.

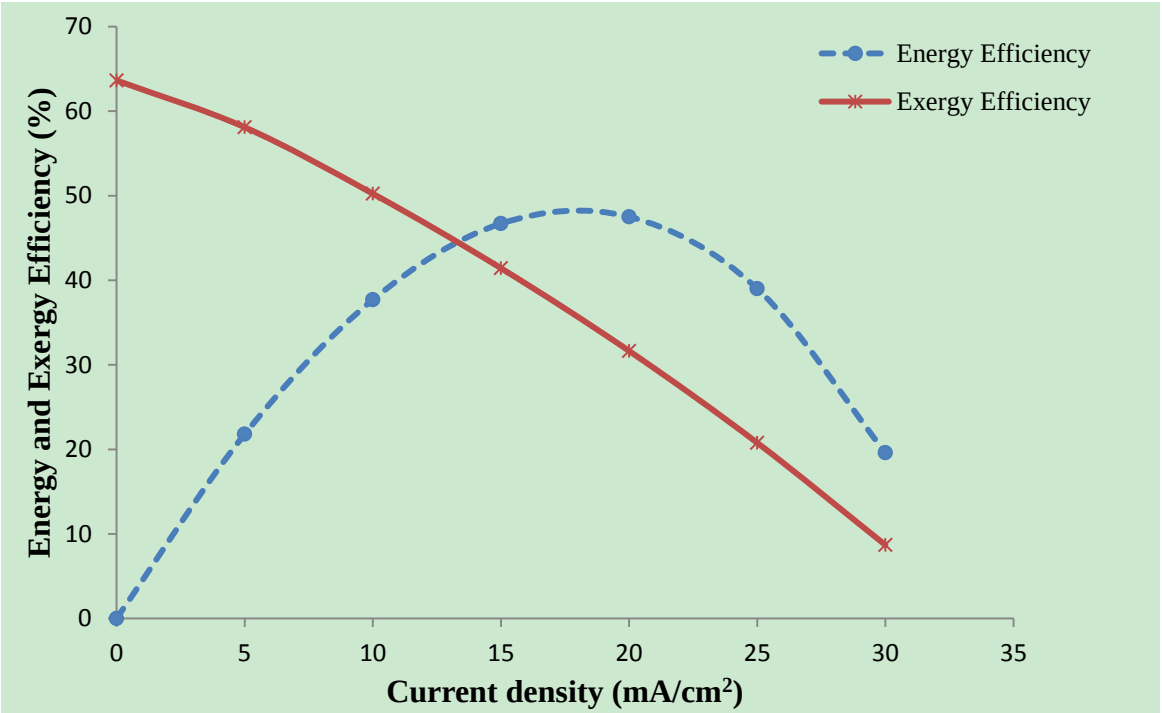

Fig. 8 Simulated influence of current density on the exergy and energy performance of DMFC

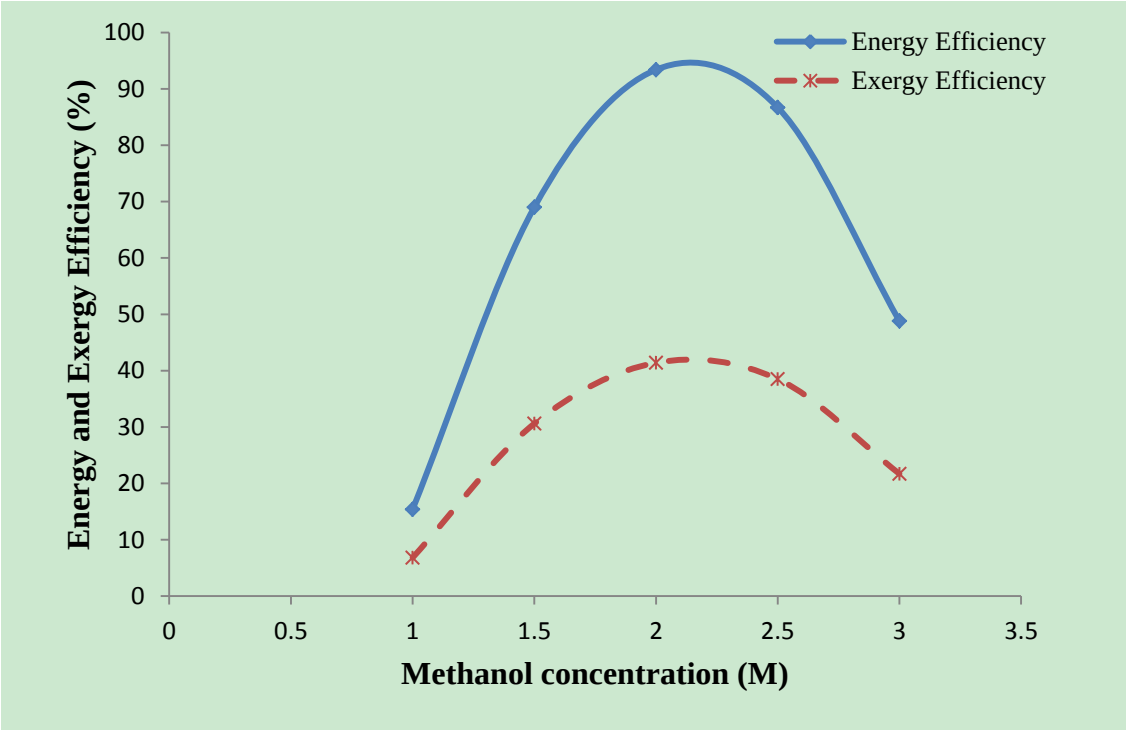

Fig. 9 Effects of methanol concentration on energy and exergy efficiencies of DMFC

This study also simulated the influence of methanol concentration on the energy and exergy efficiencies of direct methanol fuel cells. The results are presented in Fig. 9. It was discovered that both energy and exergy efficiencies increased with increases in methanol concentrations. After reaching their maximum efficiency of 93.4% energy and 41.4% exergy at 2 M methanol concentration, further increments in the methanol concentration resulted in reductions of both the exergy and energy efficiencies. At higher fuel (methanol) concentrations there was an excess of methanol in the cell, which lead to methanol crossover through the membrane, consequently leading to a reduction in cathode potential and reduction in the cell

DOI: 10.5963/AMSA0403001

performance [11]. It was inferred from various results of this study that the predictive mathematical model could be used to predict the performance of DMFCs at different operating conditions.

IV. CONCLUSIONS

This study focused on the development of a predictive mathematical model for energy and exergy analyses of direct methanol fuel cells. The model was investigated using computer simulation, and the results revealed that the operating temperature of 353 K, anode and cathode pressures of 15 atmosphere, and methanol concentration of 2 M produced the cell best performance. It was therefore deduced from the simulated results that the developed mathematical model could be utilized to predict cell performance under different operating conditions.

ACKNOWLEDGMENTS

University Board of Research (UBR), Step B Project of the Federal University of Technology Minna, Nigeria and Botswana International University of Science and Technology (BIUST) are appreciated for their financial and technical supports.

REFERENCES

[1] E. B. Edward, *A short course in organic chemistry*, Russia, MW: Mir Press, 2001.

[2] K. Sopian and W. J. Wan Daud, "Challenges and future developments in proton exchange membrane fuel cells," *Renewable Energy*, vol. 31, pp. 719-727, 2006.

[3] A. B. J. Stambouli, "Solid oxide fuel cells (SOFCs)," *Environ. Clean & Eff. Source Energy, Renewable & Sustainable Energy Review*, vol. 6, pp. 433-455, 2002.

[4] T.P. Kevin and A. O. Lewis, *An introduction to global environment issue*s, United Kingdom, LD: Bulter Tanner, 2001.

[5] T. Yachi, M. Shibasaki, and T. J. Tatsui, "A new direct methanol fuel cell with a zigzag folded membrane electrode assembly," *Power Source*, vol. 145, pp. 477-484, 2005.

[6] Y. Gubb, G. P. Robertson, M. D. Guiver, X. Jian, D.M. Serguei, K. Wang, and S. J. Kaliguine, "Sulfonation of poly (phthalaziones) with fuming sulfuric acid mixtures for proton exchange membrane materials," *Membr. Sci.*, vol. 227, pp. 39-50, 2003.

[7] M. K. Song, Y. T. Kim, and J. M. J. Fentom, "Chemically modified nation/poly (vinylidene fluoride) blend ionomers for proton exchange membrane fuel cells," *Polymer Sci.*, vol. 117, pp. 114-121, 2003.

[8] S. Wang, G. Sun, G. Wang, X. Zhao, H. Sun, X. Fam, B. Yi, and Q. Xin, "Improvement of direct methanol fuel cell performance," *Electrochem. Comm.*, vol. 7, pp. 1007-1012, 2005.

[9] S. Song, S. Dovatzides, and P. J. Tsiakars, "Energy analysis of an ethanol fuelled proton exchange membrane fuel cell system for automobile applications," *Power Source*, vol. 145, pp. 123-134, 2005.

[10] S. O. B. Shrestha and S. Mohan, "Performance and modelling of a direct methanol fuel cell," Proc. World Congress on Eng. III. United States of America, New York, McGrew-Hill, 2011.

[11] K. Ayoub and A. Kazim, "Exergy analysis of a PEM fuel cell at variable operating conditions," *Energy Conv. & Manag.*, vol. 45, pp. 1949-1961, 2004.

[12] G.Q. Lu and C. Y. J. Wang, "Electrochemical and flow characterization of a direct methanol fuel cell," *Power Sources*, vol. 134, pp. 33-40, 2004.

[13] A.O.E. Neja, K. Segighi, M. Farbadi, and F. J. Asghari, *World Applied Sciences*, vol. 31, iss. 10, pp. 1847-1856, 2014.

[14] Y.S. Jin and T. V. J. Nyuyen, "Multi-component transport in porous electrode of proton exchange membrane fuel cells using the inter digitated gas distribution," *Electrochem. Soc*., vol. 146, pp. 38-45, 2000.

[15] I. Parsons, *Fuel cell handbook*, United States of America, NY: EGG services, 2000.

[16] H. K. Ozturk, I. Dincer, and A. Yilanci, "Performance analysis of a PEM fuel cell unit in a solar-hydrogen system," *Inter. J. Hydrogen Energy*, vol. 33, pp. 7538-7552, 2008.

[17] K. Badyda, J. Milewski, and A. Miller, "The control strategy for high temperature fuel cell hybrid system," *J. Electro. & Elect Eng.*, vol. 2, pp. 381-390, 2011.

[18] R. B. Bird, W. E. Stewart, and E. N. Lightfoot, *Transport Phenomena*, 2nd ed., New York, United States, John Wiley and Sons, 2002.

[19] A. R. Maher and A. J. Sadiq, "Modelling of proton exchange membrane fuel cell performance based on semi-empirical equations," *Renewable Energy*, vol. 30, pp. 1587-1599, 2005.

[20] T. Uma, "Non linear state estimation in polymer electrolyte membrane fuel cells," United States, DT: Cleveland Press, 2008.

DOI: 10.5963/AMSA0403001